NASA/CR—2004-213101 ARL–CR–0540

New Design and Improvement of Planetary Gear Trains

Faydor L. Litvin, Alfonso Fuentes, Daniele Vecchiato, and Ignacio Gonzalez-Perez
University of Illinois at Chicago, Chicago, Illinois

July 2004

The NASA STI Program Office . . . in Profile

Since its founding, NASA has been dedicated to the advancement of aeronautics and space science. The NASA Scientific and Technical Information (STI) Program Office plays a key part in helping NASA maintain this important role.

The NASA STI Program Office is operated by Langley Research Center, the Lead Center for NASA's scientific and technical information. The NASA STI Program Office provides access to the NASA STI Database, the largest collection of aeronautical and space science STI in the world. The Program Office is also NASA's institutional mechanism for disseminating the results of its research and development activities. These results are published by NASA in the NASA STI Report Series, which includes the following report types:

- TECHNICAL PUBLICATION. Reports of completed research or a major significant phase of research that present the results of NASA programs and include extensive data or theoretical analysis. Includes compilations of significant scientific and technical data and information deemed to be of continuing reference value. NASA's counterpart of peer-reviewed formal professional papers but has less stringent limitations on manuscript length and extent of graphic presentations.

- TECHNICAL MEMORANDUM. Scientific and technical findings that are preliminary or of specialized interest, e.g., quick release reports, working papers, and bibliographies that contain minimal annotation. Does not contain extensive analysis.

- CONTRACTOR REPORT. Scientific and technical findings by NASA-sponsored contractors and grantees.

- CONFERENCE PUBLICATION. Collected papers from scientific and technical conferences, symposia, seminars, or other meetings sponsored or cosponsored by NASA.

- SPECIAL PUBLICATION. Scientific, technical, or historical information from NASA programs, projects, and missions, often concerned with subjects having substantial public interest.

- TECHNICAL TRANSLATION. English-language translations of foreign scientific and technical material pertinent to NASA's mission.

Specialized services that complement the STI Program Office's diverse offerings include creating custom thesauri, building customized databases, organizing and publishing research results . . . even providing videos.

For more information about the NASA STI Program Office, see the following:

- Access the NASA STI Program Home Page at ***http://www.sti.nasa.gov***

- E-mail your question via the Internet to help@sti.nasa.gov

- Fax your question to the NASA Access Help Desk at 301–621–0134

- Telephone the NASA Access Help Desk at 301–621–0390

- Write to:
  NASA Access Help Desk
  NASA Center for AeroSpace Information
  7121 Standard Drive
  Hanover, MD 21076

NASA/CR—2004-213101 ARL–CR–0540

New Design and Improvement of Planetary Gear Trains

Faydor L. Litvin, Alfonso Fuentes, Daniele Vecchiato, and Ignacio Gonzalez-Perez
University of Illinois at Chicago, Chicago, Illinois

Prepared under Grant NAG3–2450

National Aeronautics and
Space Administration

Glenn Research Center

July 2004

Available from

NASA Center for Aerospace Information
7121 Standard Drive
Hanover, MD 21076

National Technical Information Service
5285 Port Royal Road
Springfield, VA 22100

Available electronically at http://gltrs.grc.nasa.gov

New Design and Improvement of Planetary Gear Trains

Faydor L. Litvin, Alfonso Fuentes, Daniele Vecchiato, and Ignacio Gonzalez-Perez
University of Illinois at Chicago
Chicago, Illinois 60607-7022

Summary

The development of new types of planetary and planetary face-gear drives is proposed. The new designs are based on regulating backlash between the gears and modifying the tooth surfaces to improve the design. The goal of this work is to obtain a nearly uniform distribution of load between the planet gears. In addition, a new type of planetary face-gear drive was developed in this project.

Research Program

New types of Planetary Face-Gear Drives

The developed face-gear drives are shown in figs. 1, 2, and 3. The research program covers basic ideas of the design of the proposed gear drives.

Fig. 1 shows a planetary face-gear drive formed by coaxial face-gears 1 and 4, and two rigidly connected helical gears 2 and 3, mounted on the carrier. A crossing angle γ is formed by axes of face-gears 1 and 2 that differs from 90°.

The advantages of the proposed gear trains are as follows:

(i) A high gear ratio may be easily achieved. However, the high gear ratio will be accompanied with lower efficiency. A graph that shows the relation between the efficiency of the train and the gear ratio will be presented later.

(ii) The gear train mentioned above can also be used as a differential. In comparison with a differential train formed by spiral bevel gears, the meshing and precision will be substantially improved due to separate meshing of two pairs of gears: gear 1 and 2, gears 3 and 4. In a train of spiral bevel gears, the same planet gear is simultaneously in mesh with two other spiral bevel gears. The simultaneous meshing of three bevel gears is a substantial obstacle for optimization of meshing.

(iii) The technology of gears of a face-gear drive is simpler in comparison to that of the spiral bevel gears.

A new method of generation of face-gears by grinding, performed by application of a worm of special shape, will be developed. Such a worm may be applied as a cutting tool (hob). The grinding worm and the shaper may be used for generation of the face-gear. This new technology for face-gear manufacture, permits the application of hardened materials.

The face-gear drives shown in figs. 2 and 3 can be successfully applied for torque splitting. Fig. 2 shows an example of an angular transmission wherein the input torque, applied to floating

pinion 1, is split between gears 2 and 3. Then gear 4 transfers the torque from gear 3 back to gear 2. The advantages of such a transmission are as follows:

(i) The floating pinion 1 allows a very precise torque splitting, therefore such a mechanism may double the transmitted torque in comparison with the mechanism formed only by gears 1 and 2.

(ii) The meshing of face-gears 2 and 3 with pinion 1 is not sensitive to the axial displacement of pinion 1. In comparison with spiral bevel gears, installation of gears is simplified and compensation of thermal extensions of shaft 1 is provided automatically.

(iii) Face-gear drives can obtain a high transmission ratio: reductions of 5 to 10 for a single stage becomes possible.

The gear drive shown in fig. 3 is formed by: (i) coaxial face gears 1 and 3, and (ii) carrier c at which are mounted N_p planets 2^i, $i = 1,\ldots,N_p$. Spur or helical gears may be utilized. Extended axial dimensions of planets 2^i are required for simultaneous meshing of face-gears 1 and 3. Each planet is rotated independently with respect to the carrier.

The advantage of this gear train is the possibility to obtain a low gear ratio, that is not permissible by a conventional face-gear train.

The design of a face-gear drive requires: (i) avoidance of singularities and tooth pointing by generation of a shaper, and (ii) avoidance of singularities of the generating worm. Methods for solution of the problems mentioned above and developments of respective computer programs are accomplished in this paper.

One-Stage Planetary Gear Train

The schematic of a conventional planetary gear train is shown in fig. 4. The main goal is obtaining a more uniform load distribution between the planet gears. For this purpose: (i) helical gears (of a small helix angle) will be used instead of spur gears, (ii) the tooth surfaces will be modified in comparison with conventional ones (fig. 5).

The new design will permit the: (i) regulation of backlash for achievement of almost uniform load distribution, and (ii) reduction of transmission errors caused by misalignment.

The regulation of backlash will be achieved by providing a small screw motions of the planet gears in the process of assembly. Fig. 6 illustrates schematically the effect of regulation of backlash.

Reduction of transmission errors will be achieved by the application of a predesigned parabolic function of transmission errors that can adsorb linear functions of transmission errors caused by misalignments. Fig. 7 illustrates schematically that functions of transmission errors and backlash are different for subgear drives formed by various planet gears and therefore the load between planet gears cannot be distributed uniformly. (A subgear drive is formed by a ring gear, sun gear, and a sole planet gear).

However, the proposed approach of regulating the installment of planet gears permits an integrated function of reduced transmission errors and a minimized backlash magnitude (fig. 8) can be obtained.

In fig. 5 a one-stage planetary gear train with double-helical gears is shown. Such a gear drive is an example of a complicated multi-body system, for which it is difficult to obtain a

uniform (or almost uniform) load distribution between the planet gears. An approach for simple regulation of the backlash between the planet gears will be developed.

1. General Considerations

1.1 Introduction

Although the working principle of planetary gears has been known for many years, there is still a great interest towards this particular device. Machine designers that work in many different fields are attracted by this mechanisms because they successfully solve specific problems.

Planetary gear drives are constituted by three main elements: (i) a sun gear, (ii) a carrier that hosts planet gears, and (iii) a ring gear. Either the sun or ring gears may be fixed, the other performs rotation about its axis (fig. 4). The planet gears perform rotation with the carrier and about the carrier (fig. 4).

There are three main configurations for application of a planetary gear. The gear train may have:

(i) one input, one output, and one fixed element. The input shaft may be a sun or the carrier, the output is the remaining element. In this case the mechanism is a speed reducer (or multiplier)

(ii) one input, two outputs, and no fixed element. The input shaft may be the carrier, the outputs the sun and ring gears. In this case the mechanism is a differential. The output torque is divided among the two output shafts

(iii) two inputs, one output, and no fixed element. This mechanism is a speed combiner, since the output speed is a linear combination of the speed of the two input shafts.

There are even some more applications where the configuration of the system may be changed during the operation. Planetary gear drive of fig. 4, for instance, can be applied as a two-speed transmission. The input shaft is the central sun gear 1, and the output shaft is the carrier *c*. The first speed is obtained keeping gear 3 at rest. Then, the second speed is obtained connecting gear 3 to the input shaft (direct drive).

Another key point for flexibility of the design is the application of various gear types: spur, helical and double helical gears are examples of commonly applied technologies. Straight bevel gears are widely applied in automotive differentials. Application of face-gear drives is a new possibility that has recently been achievable since the development of enhanced face-gear manufacturing technology. Examples of such application for a reducer and a differential are provided in this report.

Besides the advantages that come from the enormous flexibility of design that planetary gear trains allow, there are several other positive aspects related with the application of such mechanism. The most evident advantage in comparison with conventional gear drives is that the power entering the mechanism is branched out through many planetary gears. This reduces substantially the load carried by each contacting pair of teeth, making possible the adoption of smaller tooth dimensions. In turn, this results in design of smaller dimensions of the gears and reduced peripheral speed (pitch line velocity).

Another advantage is a higher gear ratio of the planetary gear drive in comparison with the inverted train (see definition of inverted train in section 1.3). With reference to fig. 4, suppose that the input shaft is gear 1 and the output shaft is the carrier. The gear ratio will be:

$$\frac{\omega_c}{\omega_1} = \frac{N_1}{N_1 + N_3} \tag{1.1}$$

Consider now an inverted train formed by gears 3 and 1 wherein the carrier *c* is fixed. Gear 3 is the output one, and the gear ratio is:

$$\frac{\omega_3}{\omega_1} = \frac{N_1}{N_3} \tag{1.2}$$

Here, the negative sign indicates that links 1 and 3 rotate in opposite directions.

Comparing the angular velocities of the output link that is provided by equations (1.1) and (1.2), we will find out that the planetary gear drive provides a larger reduction of the speed of the output link. Application of planetary gear drives can result in a fewer number of stages for a given speed reduction.

The efficiency of planetary gear trains plays also an important role. Deriving the efficiency of the planetary gear train of fig. 4 in the case that link 3 is held at rest (see section 1.3), it is possible to prove that the efficiency of the planetary train is always higher than the efficiency of the inverted train. The previous statement is always true: the fact that the input link is the sun gear or the carrier doesn't change this conclusion. However, gear ratio provided by this mechanism is usually less than six to one per stage.

Other planetary gear trains, like the one shown in fig. 1, may be designed to provide much higher gear ratios (see below). However, a price is paid for this by reduced efficiency.

One of the limiting factors for high speed applications of planetary gear trains is the angular speed of the carrier. This limitation exists because of the centrifugal load (due to the inertia of planetary gears) that affects the bearings of the carrier. Some aerospace high speed applications make use of a gear drive similar to fig. 4, but with the carrier held at rest.

A problem that is faced by all the designers of planetary gear trains is the determination of the load acting on each planet. The difficulty comes from the fact that a planetary gear train is an hyper static multi-body system, therefore the load acting on each member is not easily determined.

In the case of ideal manufacturing and assembly, the assumption of the load being equally split is reasonable. However, in a general case errors of manufacturing and assembly have to be considered. In this case, assuming that the train is constituted by rigid bodies, only a single planetary gear will be simultaneously in mesh with gears 1 and 3.

In reality, since the links that constitute the mechanism are deformable, by progressive application of the load an increasing number of members will be in mesh. However, the first planetary gear that was in mesh after application of the load will carry a higher load. The disadvantage of non uniform load distribution can be effectively reduced by regulation of installment of planet gear as it is proposed in this report (fig. 6).

1.2 Gear Ratio

The gear ratio (section 1.2) and the efficiency of a planetary gear train (section 1.3) are determined by application of the idea of an *inverted* gear train formed by the gears of the planetary mechanism [1].

The carrier of the inverted mechanism is considered as fixed. The inversion is based on the idea that the gears of both mechanisms, the planetary and the inverted one, perform rotations about the carrier with the *same* angular velocity.

The angular velocities of the links of the planetary mechanism are related by the following equation [2]:

$$\frac{\omega_k - \omega_c}{\omega_1 - \omega_c} = m_{12}^{(c)} \tag{1.3}$$

Here, ω_k is the angular velocity of gear k in absolute motion with respect to the frame of the planetary mechanism; ω_k-ω_c is the angular velocity of gear k in its relative motion with respect to the carrier; $m_{k1}^{(c)}$ is the gear ratio of the inverted mechanism wherein the transformation of motion is performed from gear k to gear 1 while the carrier is held at rest. The gear ratio $m_{k1}^{(c)}$ is considered as an algebraic quantity: $m_{k1}^{(c)}$ is negative ($m_{k1}^{(c)}<0$) if the direction of rotation from gear 2 to gear 1 of the inverted mechanism is opposite. Similarly, ratio $m_{k1}^{(c)}$ is positive wherein directions of rotation of gears k and 1 of the inverted mechanism coincide.

We illustrate application of eq. (1.3) for the gear drive shown in fig. 1. Assume that face-gear 4 is fixed ($\omega_k = \omega_4 = 0$) and the train is used as a planetary one. Then we obtain

$$-\frac{\omega_1 - \omega_c}{\omega_c} = m_{12}^{(c)} \cdot m_{34}^{(c)} = (-1)\frac{N_2}{N_1}(-1)\frac{N_4}{N_3} \tag{1.4}$$

Equation (1.4) yields

$$m_{c1}^{(4)} = \frac{\omega_c}{\omega_1} = \frac{1}{1 - \dfrac{N_2 N_4}{N_1 N_3}} = \frac{N_1 N_3}{N_1 N_3 - N_2 N_4} \tag{1.5}$$

Here: ω_c and ω_1 are the angular velocities of rotation of carrier c and face-gear 1; $m_{c1}^{(4)}$ is the gear ratio of the train where carrier c and face-gear 1 are the driving and driven members of the gear train and gear 4 is held at rest; N_i (i = 1,...,4) is the tooth number.

In the case where $N_2 = N_3$, we obtain that

$$m_{c1}^{(4)} = \frac{N_1}{N_1 - N_4} \tag{1.6}$$

A substantial reduction of angular velocity ω_c may be obtained. However, the efficiency of the train depends substantially on the applied gear ratio $m_{c1}^{(4)}$.

1.2.1 Numerical Example.—The train of fig. 1 is formed as follows: output gear N_1 = 100, planet gears $N_2 = N_2 = 17$, fixed gear $N_4 = 88$, crossing angle $\gamma = 75°$, helix angle $\beta = 10°$.

The helix angles of pinions 2 and 3 are of the same directions in order to reduce the axial load on the carrier c transformed from the pinions.

It follows from eq. (1.6) that

$$m_{c1}^{(4)} = \frac{\omega_c}{\omega_1} = \frac{100}{100-88} = 8.333 \tag{1.7}$$

Such a gear ratio is obtained for a gear train that performs rotation between coinciding axes. However, this arrangement has a comparatively low efficiency that will be shown later (see section 1.3).

1.2.2 Numerical Example.—A gear train that is used in helicopter transmissions (see fig. 4) will be assessed. Gear 3 (ring gear) is fixed and the carrier *c* caries *n* planet gears (*n* = 5 is shown in fig. 4). Equation (1.3) yields

$$\frac{\omega_1 - \omega_c}{-\omega_c} = m_{13}^{(c)} \tag{1.8}$$

Here, $m_{13}^{(c)}$ is the gear ratio of the inverted mechanism

$$m_{13}^{(c)} = m_{12}^{(c)} \cdot m_{23}^{(c)} = (-1)\frac{N_2}{N_1}(+1)\frac{N_3}{N_2} = (-1)\frac{N_3}{N_1} \tag{1.9}$$

Equations (1.8) and (1.9) yield

$$\frac{\omega_c}{\omega_1} = \frac{N_1}{N_1 + N_3} \tag{1.10}$$

The reduction of angular velocity, ω_c, is obtained where gear 1 and carrier *c* are the driving and driven links, respectively.

Note: The number of planet gears and tooth numbers of gears 1 and 3 are related as follows [1]: $\frac{N_1 + N_3}{n_p}$ has to be an integer number, where n_p is the number of planet gears.

1.3 Efficiency of a Planetary Gear Train

Let us compare a planetary gear train with a conventional one, with fixed gear axes, designed for the same gear ratio of angular velocities of the input and output mechanism links. The comparison shows the following [7]:

(i) The planetary gear train has smaller dimensions than the conventional one. In a conventional design a set of gear drives is required, not a single train for the required speed reduction.

(ii) However, the planetary gear train has usually a much lower efficiency in comparison with the conventional gear train. An exception is the planetary gear train shown in fig. 4 (see Example 1.3.2).

The determination of the efficiency of a planetary gear train is a complex problem. A simple solution to this problem is proposed by [3] (see as well [1]) and is based on the following considerations:

(i) The efficiency of the planetary gear train is related with the efficiency of the inverted train wherein the relative velocity of the planetary train and the inverted one is observed as the same. The inverted train is obtained from the planetary train wherein the carrier is held at rest and gear *j*, that has been fixed in the planetary train, is released.

(ii) Two cases of efficiency of planetary train designated by $\eta_{ic}^{(j)}$ and $\eta_{ci}^{(j)}$ might be considered. Here designations in $\eta_{ic}^{(j)}$ indicate that gear *i* and carrier *c* are the driving and driven links of the planetary train. Respectively, designations in $\eta_{ci}^{(j)}$ indicate that carrier *c* and gear *i* are the driving and driven links of the planetary train. In both cases, the superscript (*j*) indicates that gear *j* is the fixed one.

(iii) We consider gear *i* or carrier *c* as the driving link of the planetary gear train if

$$M_k \omega_k > 0, \quad (k = 1, c) \tag{1.11}$$

where M_k is the torque applied to link *k*; ω_k is the angular velocity of link *k* in absolute motion, in rotation about the frame of the planetary gear train.

(iv) It is assumed that a torque M_i of the same magnitude is applied to link *i* of the planetary and inverted gear trains. Torque M_i is considered as positive if *i* (but not *c*) is the driving link. In the case that the driving link is the carrier, torque M_i is the resisting moment and $M_i < 0$.

The ratio (ω_c/ω_1) may be obtained from the kinematics of the planetary gear train using the following equation for the train with fixed gear *j*:

$$\frac{\omega_1 - \omega_c}{-\omega_c} = m_{ij}^{(c)} \tag{1.12}$$

The determination of efficiency of planetary gear trains is considered for two typical examples. The approach discussed may be extended and applied for various examples of planetary gear trains.

1.3.1 Numerical Example.—Planetary gear train shown in fig. 4 is considered for the following conditions: (i) gear 3 is fixed ($j = 3$); (ii) gear 1 and carrier *c* are the driving and driven links, respectively.

Equation (1.12) yields

$$\frac{\omega_c}{\omega_1} = \frac{N_1}{N_3 + N_1} \tag{1.13}$$

Consider now the inverted gear train where rotation is provided from gear 1 to gear 3 wherein the carrier is fixed. Torque M_1 is applied to gear 1 and M_1 is positive since gear 1 is the driving gear in the planetary gear train. The angular velocity ω_1 of gear 1 of the planetary gear train is of the same direction as M_1 and $M_1\omega_1 > 0$.

The efficiency $\eta_{1c}^{(3)}$ of the planetary train is determined as

$$\eta_{1c}^{(3)} = \frac{M_1\omega_1 - P_l}{M_1\omega_1} \tag{1.14}$$

Here: $M_1\omega_1 - P_l$ is the output power, and $M_1\omega_1$ is the input power ($M_1\omega_1 > 0$).

The key for determination of $\eta_{1c}^{(3)}$ is that the power P_l lost in the *planetary* gear train is determined as the power lost in the *inverted* train. The input power of the inverted train is $M_1(\omega_1-\omega_c) > 0$, since $M_1 > 0$ and $(\omega_1-\omega_c) > 0$.

We consider as known the coefficient $\psi^{(c)} = 1 - \eta^{(c)}$ of the inverted train. Then, we may determine the power lost in the inverted gear train as

$$P_l = \psi^{(c)} M_1(\omega_1 - \omega_c) \tag{1.15}$$

Equations (1.13), (1.14), and (1.15) yield

$$\eta_{1c}^{(3)} = 1 - \psi^{(c)}\left(\frac{N_3}{N_1 + N_3}\right) \tag{1.16}$$

Rearranging terms of equation (1.15) and using the definition of $\psi^{(c)}$, it is easy to obtain the following one:

$$(1-\eta_{1c}^{(3)}) = (1-\eta^{(c)})\frac{N_3}{N_1 + N_3} \tag{1.17}$$

It is easy to notice that $\frac{N_3}{N_1 + N_3}$ is always less than one. It follows

$$(1-\eta_{1c}^{(3)}) < (1-\eta^{(c)}) \tag{1.18}$$

and

$$\eta_{1c}^{(3)} > \eta^{(c)} \tag{1.19}$$

Inequality (1.19) holds for any teeth number N_1 and N_3.

1.3.2 Numerical Example.—The same planetary gear train is considered for the conditions that the driving and driven links of the planetary gear train are the carrier and link 1, respectively.

Gear 1 is now the driven link of the planetary gear train, $M_1 < 0$ since M_1 is the resisting moment. We consider now the inverted train taking into account that $M_1(\omega_1-\omega_c) < 0$, since $M_1 < 0$, $(\omega_1-\omega_c) > 0$.

The power P_l lost in the inverted train is determined as follows

$$P_l = \frac{1}{\eta^{(c)}}(-M_1)(\omega_1 - \omega_c) - (-M_1)(\omega_1 - \omega_c) = \frac{1-\eta^{(c)}}{\eta^{(c)}}(-M_1)(\omega_1 - \omega_c) \tag{1.20}$$

Equation (1.20) provides that the lost power P_l is positive. (Recall that $M_1 < 0$ and $(\omega_l - \omega_c) > 0$).

Then we obtain

$$\eta_{c1}^{(3)} = \frac{P_{driven}}{P_{driven} + P_l} = \frac{-M_1\omega_1}{-M_1\omega_1 + \frac{1-\eta^{(c)}}{\eta^{(c)}}(-M_1)(\omega_1 - \omega_c)}$$

$$= \frac{1}{1 + \frac{1-\eta^{(c)}}{\eta^{(c)}}\left(1 - \frac{\omega_c}{\omega_1}\right)} = \frac{1}{1 + \frac{1-\eta^{(c)}}{\eta^{(c)}}\left(\frac{N_3}{N_1 + N_3}\right)} \tag{1.21}$$

Equation (1.21) may be rearranged as follows:

$$\frac{1-\eta_{c1}^{(3)}}{\eta_{c1}^{(3)}} = \frac{1-\eta^{(c)}}{\eta^{(c)}}\frac{N_3}{N_1 + N_3} \tag{1.22}$$

Following the same procedure as in the Example 1.3.1, we recognize that $\frac{N_3}{N_1 + N_3} < 1$, therefore:

$$\frac{1-\eta^{(c)}}{\eta^{(c)}} > \frac{1-\eta_{c1}^{(3)}}{\eta_{c1}^{(3)}} \tag{1.23}$$

Simplifying inequality (1.23) the following is obtained:

$$\eta_{c1}^{(3)} > \eta^{(c)} \tag{1.24}$$

Inequalities (1.19) and (1.24) prove that the efficiency of the planetary gear train shown in fig. 4 is always higher than the efficiency of the corresponding inverted train.

1.4 New Geometry of Face Gear Drives

The existing geometry of face gear drives is based on application of a spur involute pinion. The generation of the face gear is based on application of a spur involute shaper. The tooth number N_s of the shaper is increased in comparison with the tooth number N_1 of the pinion for bearing contact localization. The disadvantage of the existing geometry is the possibility of areas with severe contact stresses. The bearing contact is oriented across the surface.

The new geometry of face gear drives is based on following ideas:

(i) Two rack-cutters Σ_{c1} and Σ_{cs} of parabolic profiles are used during the generation of the shaper and the pinion respectively (figs. 9(b) and 9(c)).

(ii) Rack-cutters Σ_{c1} and Σ_{cs} are provided with *mismatched* parabolic profiles that *deviate* from the straight line profiles of the reference rack-cutter Σ_c (fig. 9(a)).

Skew rack-cutters with parabolic profiles may be also applied. Such rack cutters might be applied for generation of helical pinions and shapers. The helix angle of the pinion should be less than 15° if the pinion is ground by a worm of a special shape (see below). The advantage of helical pinions, of the new geometry, is the ability to obtain a longitudinal bearing contact and increase the contact ratio.

1.5 Grinding of Face Gears

Grinding or cutting of face gears may be performed by a worm of special of special shape with a limited number of threads (fig. 10). Design of such a worm requires avoidance of surface singularities [4]. Locations of singularities are schematically noted in area A (fig. 10).

The idea of design of a worm for generation of face-gears is based on simultaneous meshing of the worm and the shaper with the face-gear being generated (fig. 11). It is considered in such an approach that the shaper is in line contact between the face-gear and the worm is in point contact with the face gear. The whole surface of the face-gear is generated due to application of two-parameter enveloping process wherein the worm performs a feed motion as the screw motion about the axis of the shaper with the screw parameter of the shaper.

1.6 Stress Analysis

A stress analysis, based on finite element method [5] and application of a general purpose FEA computer program [6] has been developed. The main difference of the stress analysis performed from previous methods is that the derivation of contact model (fig. 12) is determined analytically using the equations of tooth surfaces [7].

2. New Types of Planetary Face Gear Drives

2.1 Description of Developed Face Gear Drives

2.1.1 Gear Train 1.—The gear train is formed (fig. 1): (i) by coaxial face gears 1 and 4, and (ii) carrier *c* at which are mounted helical pinions 2 and 3. Pinions 2 and 3 are rigidly connected and perform: (a) transfer motion with carrier *c*, and (b) relative motion about carrier. The helix angles of pinions 2 and 3 are of the same directions in order to reduce the axial load on carrier *c* transformed from the pinions.

Assume that face-gear 4 is fixed and the train is used as a planetary one. It follows from the kinematics of the train that

$$-\frac{\omega_1-\omega_c}{\omega_c}=m_{12}^{(c)}\cdot m_{34}^{(c)}=(-1)\frac{N_2}{N_1}(-1)\frac{N_4}{N_3} \tag{2.1}$$

Then, we obtain

$$m_{c1}^{(4)}=\frac{\omega_c}{\omega_1}=\frac{1}{1-\frac{N_2N_4}{N_1N_3}}=\frac{N_1N_3}{N_1N_3-N_2N_4} \tag{2.2}$$

Here: ω_c and ω_1 are the angular velocities of rotation of carrier c and face-gear 1; $m_{c1}^{(4)}$ is the gear ratio of the train where carrier c and face-gear 1 are the driving and the driven members of the gear train and gear 4 is held at rest; N_i (i = 1,2,3,4) is the number teeth.

In the case where $N_2 = N_3$, we obtain that

$$m_{c1}^{(4)}=\frac{N_1}{N_1-N_4} \tag{2.3}$$

A substantial reduction of angular velocity ω_c may be obtained. However, the efficiency of the train depends substantially on the applied gear ratio $m_{c1}^{(4)}$.

Note: The gear train may be applied as well as a differential considering that the driving link is the carrier and the two driven members are 1 and 4. The advantage of such a differential is that zones of meshing (between 2 and 1, between 3 and 4) are separated and this permits increasing the precision and conditions of contact.

Numerical Example 2.1.1: The gear train of fig. 1 is formed as follows: output gear N_1 = 100, planet gears $N_2 = N_3$ = 17, fixed gear N_4 = 88, crossing angle $\gamma = 75°$, helix angle $\beta = 10°$. From equation (2.3) it follows that

$$m_{c1}^{(4)}=\frac{\omega_c}{\omega_1}=\frac{100}{100-88}=8.333 \tag{2.4}$$

Determination of efficiency of such a gear train has to carefully consider the direction of rotation of the input shaft (carrier) and output shaft (gear 1). It is possible to distinguish two cases:

(i) $N_1 \cdot N_3 > N_2 \cdot N_4$: in this case, ω_c and ω_1 have the same direction of rotation.

(ii) $N_1 \cdot N_3 < N_2 \cdot N_4$: in this case, ω_c and ω_1 have opposite directions of rotation.

We will limit our attention to the case (i). Extension to case (ii) is straightforward.

Since the driving shaft of the planetary train is the carrier, $M_c > 0$. Since ω_c and ω_1 have the same direction of rotation, balance of work requires output torque $M_1 < 0$.*

Taking into account that $\omega_c > \omega_1$ for a reducer, it follows that

$$M_1(\omega_1-\omega_c)>0 \tag{2.5}$$

* The previous statement is based of the condition $M_{in}\omega_{in} + M_{out}\omega_{out} = 0$. Here, input power is positive, output power negative.

Equation (2.5) represents the *input* power of the inverted train. The lost power of the inverted train coincides with the lost power of the planetary train and is given by:

$$P_l = (1-\eta^{(c)})M_1(\omega_1 - \omega_c) \tag{2.6}$$

Equation (2.6) provides that P_l is positive.

The efficiency of the planetary train is then given by:

$$\eta_{c1}^{(4)} = \frac{P_{driven}}{P_{driven} + P_l} \tag{2.7}$$

The power of the driven link is

$$P_{driven} = -M_1\omega_1 > 0 \tag{2.8}$$

Substituting (2.6), (2.8) into (2.7), the final expression for the efficiency is obtained as follows:

$$\eta_{c1}^{(4)} = \frac{1}{1+(1-\eta^{(c)})\dfrac{N_2N_4}{N_1N_3+N_2N_4}} \tag{2.9}$$

Fig. 13 shows the gear ratio (eq. (2.3)) of the train and the efficiency (eq. (2.9)) as functions of the number of teeth, N_4. Values of N_i i = 1,2,3 are the same as in the example. The assumed power loss is of 2 percent at each mesh for these results. The graph highlights that high gear ratios correspond to low efficiency. For the data of this example, the expected efficiency would be about 77.5 percent.

2.1.2 Gear Train 2.—The gear train shown in fig. 2 is formed by: (i) the coaxial face gears 2 and 3, (ii) the input pinion 1, and (iii) the idler pinion 3. Pinions 1 and 3 might be helical or spur involute, or with modified profiles. The input shaft connected to pinion 1 is compliant in radial direction.

The driving torque applied to pinion 1 will be balanced by two tangential forces (generated by gears 1 and 3 respectively). Due to the high compliance of the pinion radial location, the two forces will be equal and opposite.

Torque transferred to gear 3 is then recombined in gear 2 (connected to the output shaft) by the idler pinion 4. In this way, the torque is first split and then recombined. The advantage is that the transmissible torque of the mechanism is doubled. The gear drive is not sensitive to an axial misalignment of the pinion, so the thermal expansions of the shaft are easily accommodated.

Such a mechanism can find applications where an high gear ratio, high speed and torque is required in small space. Examples are automotive and aerospace transmissions, robots and for milling machines. In comparison with spiral bevel gears, a simplified gearbox with reduced precision is required.

It is obvious that this is not a planetary mechanism. It follows from the kinematics of the train that $N_1 = N_4$ and $N_2 = N_3$. The transmission ratio is

$$\frac{\omega_2}{\omega_1} = \frac{N_2}{N_1} \tag{2.10}$$

Determination of Efficiency: Determination of efficiency of this train is performed taking into account that the torque is split in two parts at level of pinion 1. The output power $\omega_2 T_2$ will be:

$$\omega_2 T_2 = \frac{\omega_1 T_1}{2}(\eta_{12} + \eta_{13}\eta_{34}\eta_{41}) \tag{2.11}$$

Here, η_{ij} is the efficiency of the single mesh wherein gear i is the driving and j the driven member.

The overall efficiency will be

$$\eta = \frac{\eta_{12} + \eta_{13}\eta_{34}\eta_{41}}{2} \tag{2.12}$$

Numerical Example 2.1.2: The gear train of fig. 2 is formed by the following gears: $N_1 = N_4 = 19$, and $N_2 = N_3 = 120$. According to equation (2.10) it follows that

$$\frac{\omega_2}{\omega_1} = \frac{120}{19} = 6.32 \tag{2.13}$$

Using equation (2.12) and assuming an efficiency of meshing $\eta_{ij} = 0.98$ (or 2 percent power loss per gear mesh), the total efficiency of the mechanism will be:

$$\eta = \frac{0.98 + 0.98 \cdot 0.98 \cdot 0.98}{2} = 0.96 \tag{2.14}$$

2.1.3 Gear Train 3.—The gear train is formed as shown in fig. 3: (i) by coaxial face gears 1 and 3, and (ii) carrier c at which are mounted N_p planets $2^{(i)}$, $i = 1,...,N_p$. Spur or helical gears may be applied. Extended axial dimensions of planets $2^{(i)}$ are required for simultaneous mesh of face-gears 1 and 3. Each planet is rotated independently with respect to the carrier. It follows from the kinematics of the train that

$$-\frac{\omega_1 - \omega_c}{\omega_c} = m_{12}^{(c)} \cdot m_{23}^{(c)} = (-1)\frac{N_3}{N_1} \tag{2.15}$$

Thus, we obtain

$$m_{1c}^{(3)} = \frac{\omega_1}{\omega_c} = \frac{N_1 + N_3}{N_1} \tag{2.16}$$

Here, $m_{1c}^{(3)}$ is the gear ratio of the train where face-gear 1 and carrier c are the driving and the driven members of the gear train respectively. Gear 3 is held at rest.

The advantages of such a gear train are the compact dimensions. The disadvantage is that possibilities of optimization of meshing between gears 1-2 and 2-3 are reduced, since gear 2 is in mesh simultaneously with gears 1 and 3 (see below). This gear train can be used also as a differential.

Numerical Example 2.1.3: The gear train of fig. 3 is formed from the following choices of tooth numbers: output gear N_1 = 88, planet gears N_2 = 17, fixed gear N_3 = 100. From equation (2.16) it follows that

$$m_{1c}^{(3)} = \frac{\omega_1}{\omega_c} = \frac{88+100}{88} = 2.136 \tag{2.17}$$

The advantage of the planetary gear train discussed is the capability to provide a small gear ratio that cannot be obtained from a conventional face gear drive.

Such a gear drive is kinematically very similar to the gear train represented in fig. 4. The efficiency of such a gear drive may be estimated using equation (1.16). Assuming an efficiency of meshing $\eta_{12} = \eta_{23} = 0.95$, the following overall efficiency is obtained:

$$\eta_{1c}^{(3)} = 1-(1-0.95\cdot 0.95)\left(\frac{100}{88+100}\right) = 0.82 \tag{2.18}$$

The gear ratio provided by this mechanism is much lower than the one obtained, with the same gears, in example 1. However, the efficiency is fairly acceptable.

Conclusions

Based on the research conducted in this study the following conclusions can be presented:

(1) Design of a new type of face gear drives that could be applied in aircraft have been developed. Such gear drives provide: (i) application of new types of planetary gear drives with coaxial axes of input and output shafts, (ii) face gear drives with split torque, (iii) new design of a planetary face gear drive.
(2) New geometry of face gear drives based on application of parabolic rack-cutters.
(3) Generation of face-gears by a worm of a special shape.
(4) Efficiency comparison of the various gear train arrangements was performed and generally the efficiency was lower for higher gear reduction ratios.

References

[1] Litvin, F.L., Fuentes, A., *Gear Geometry and Applied Theory*, 2nd edition, Cambridge University Press, New York, 2004.
[2] Willis, R.J., *Principles of Mechanism*, Longmans, Green and Co., London, 1841.
[3] Kudrijavtzev, V.N., et al, *Computation of Design of Gear Reducers*, Politechnika S. Peterburg (in Russian), 1993.

[4] Litvin, F.L., *Gear Geometry and Applied Theory*, Prentice Hall, Inc., Englewood Cliffs, New Jersey, 1994.
[5] Zienkiewicz, O.C., and Taylor, R.L., *The Finite Element Method*, John Wiley & Sons, 5th Ed., 2000.
[6] Hibbit, Karlsson & Sirensen, Inc., *ABAQUS/Standard 6.1 User's Manual*, 1800 Main Street, Pantucket, RI 20860-4847, 1998.
[7] Argyris, J., Fuentes, A., Litvin, F.L., *Computerized Integrated Approach for Design and Stress Analysis of Spiral Bevel Gears*, Comput. Methods Appl. Mech. Engrg. 191 (2002) pp. 1057–1095.

Bibliography

Fuentes, A., Litvin, F.L., Mullins, B.R., Woods, R., Handschuh, R.F., *Design and Stress Analysis of Low-Noise Adjusted Bearing Contact Spiral Bevel Gears*, Journal of Mechanical Design, September 2002, vol. 124.

Korn, G.A. and Korn, T.M., *Mathematics Handbook for Scientist and Engineers*, McGraw-Hill, Inc., 2nd Ed., 1968.

Litvin, F.L., *Theory of Gearing*, NASA RP-1212 (AVSCOM 88-C-C035), Washington, D.C., 1989.

Litvin, F.L., *Development of Gear Technology and Theory of Gearing*, NASA Reference Publication 1406, ARL-TR-1500, 1998.

Litvin, F.L., Chen, Y.-J., Heath, G.F., Sheth, V.J., and Chen, N., *Apparatus and Method for Precision Grinding Face Gears*, USA Patent 6,146,253, 2000.

Litvin, F.L., Demenego, A., and Vecchiato, D., *Formation by Branches of Envelope to Parametric Families of Surfaces and Curves*, Computer Methods in Applied Mechanics and Engineering, vol. 190, pp. 4587–4608, 2001.

Litvin, F.L., Egelja, A.M., and De Donno, M., *Computerized Determination of Singularities and Envelopes to Family of Contact Lines on Gear Tooth Surface*, Computer Methods in Applied Mechanics and Engineering, vol. 158, no. 1–2, pp. 23–34, 1998.

Litvin, F.L., Fuentes, A., Gonzalez-Perez, I., Carnevali, L., and Sep, T.M., *New Version of Novikov-Wildhaber Helical Gears: Computerized Design, Simulation of Meshing and Stress Analysis*, Computer Methods in Applied Mechanics and Engineering, vol. 191, pp. 5707–5740, 2002.

Litvin, F.L., Fuentes, A., Zanzi, C., Matteo, P., and Handschuh, R.F., *Face Gear Drive with Spur Involute Pinion: Geometry, Generation by a Worm, Stress Analysis*, Computer Methods in Applied Mechanics and Engineering, vol. 191, pp. 2785–2813, 2001.

Litvin, F.L., Fuentes, A., Zanzi, C., Matteo, P., and Handschuh, R.F., *Design, Generation and Stress Analysis of Two Versions of Geometry of Face-Gear Drives*, Mechanism and Machine Theory 37, pp. 1179–1211, 2002.

Litvin, F.L., Seol, I. H., *Computerized Determination of Gear Tooth Surface as Envelope to Two Parameter Family of Surfaces*, Computer Methods in Applied Mechanics and Engineering, vol. 138, pp. 213–225, 1996.

Litvin, F.L., Wang, J.-C. Chen, Y.-J.D., Bossler, R.B., Heath, G.F., and Lewicki, D.J., *Face-gear drives: Design, Analysis and Testing for Helicopter Transmission Applications*, AGMA paper 92FTM2, 1992.

Litvin, F.L., Zhang, Y., Wang, J.-C., Bossler, R.B., and Chen, Y.-J.D, *Design and Geometry of Face-gear Drives*, ASME Journal of Mechanical Design, vol. 114, pp. 642–647, 1992.

Meyer, M., *Gli Ingranaggi Frontali per Applicazioni di Grande Serie*, Organi di Transmissione, Numero 5 (Prima Parte), pp. 90–98, Numero 6 (Seconda Parte), pp. 58–61, 2003.

Sheveleva, G.I., *Mathematical Simulation of Spiral Bevel Gear Production and Meshing Processes with Contact and Bending Stresses*, In Proc. IX World Congr. IFToMM, vol. 1, pp. 509–513, 1995.

Stadtfeld, H.J., *Handbook of Bevel and Hypoid Gears: Calculation, Manufacturing, and Optimization,* Rochester Institute of Technology, Rochester, New York, 1993.

Zalgaller, V.A., *Theory of Envelopes*, Publishing House Nauka (in Russian), 1975.

Zalgaller, V.A., and Litvin, F.L., *Sufficient Condition of Existence of Envelope to Contact Lines and Edge of Regression on the Surface of the Envelope to the Parametric Family of Surfaces represented in Parametric Form*, Proceedings of Universities: Mathematics (in Russian), vol. 178, no. 3, pp. 20–23, 1977.

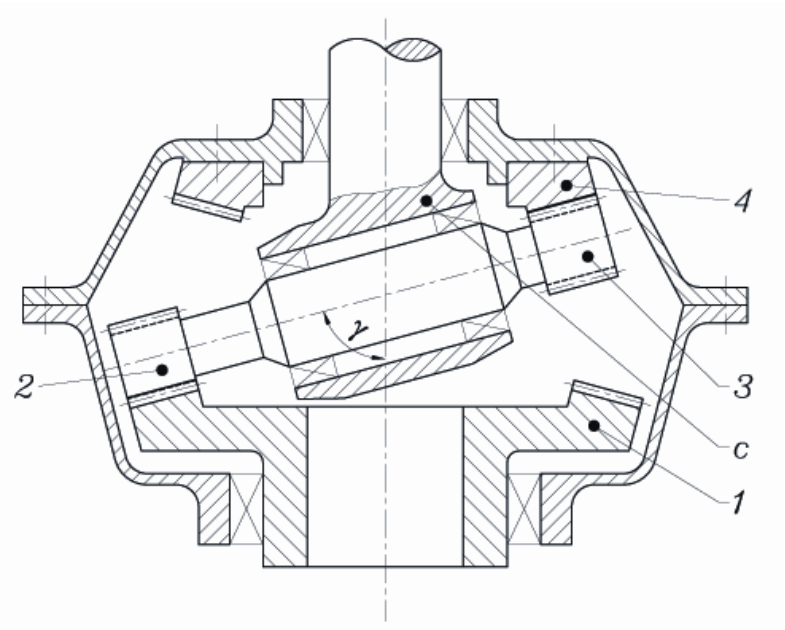

Figure 1.—Example 1: planetary face gear drive.

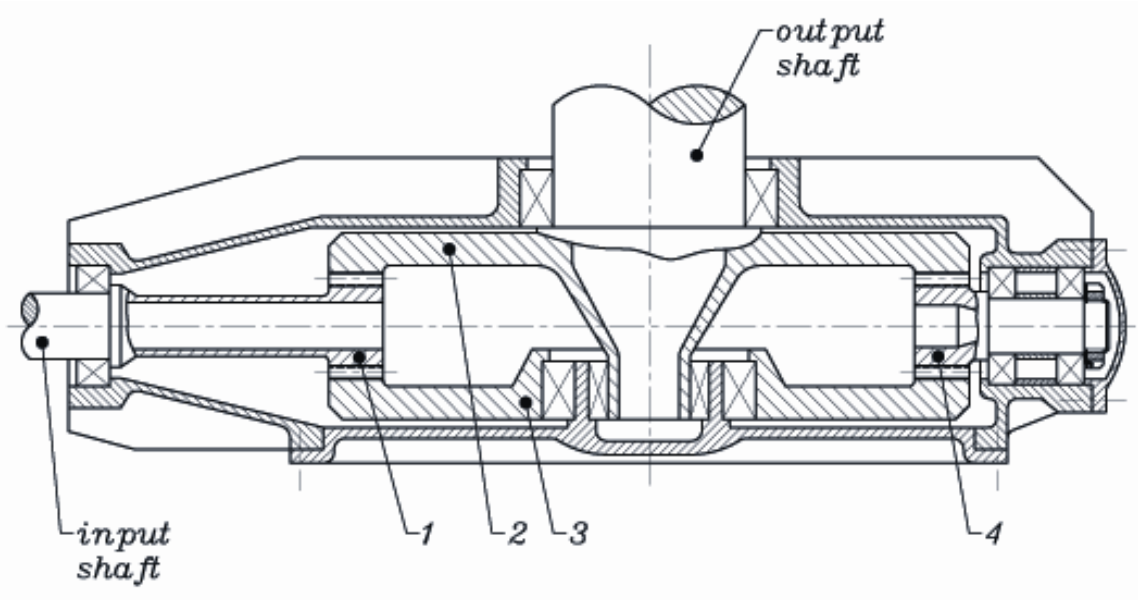

Figure 2.—Example 2: angular transmission with torque splitting.

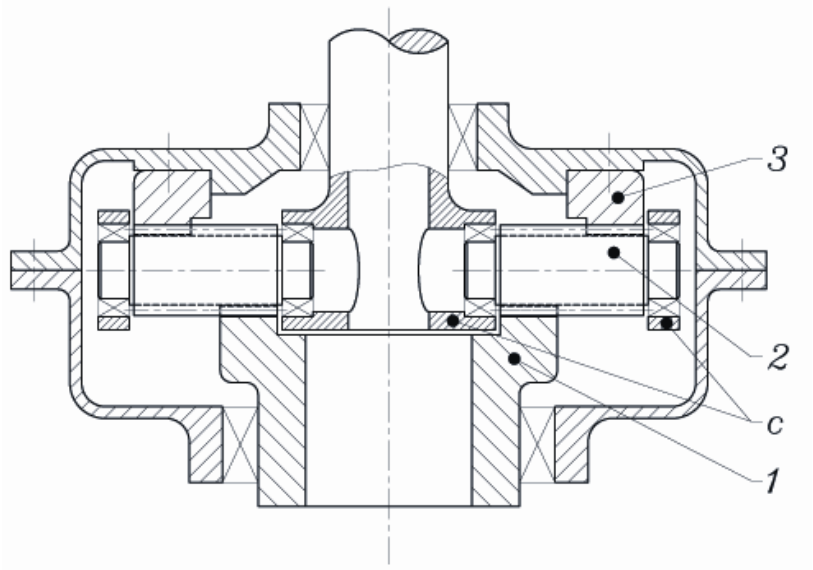

Figure 3.—Example 3: planetary face-gear drive.

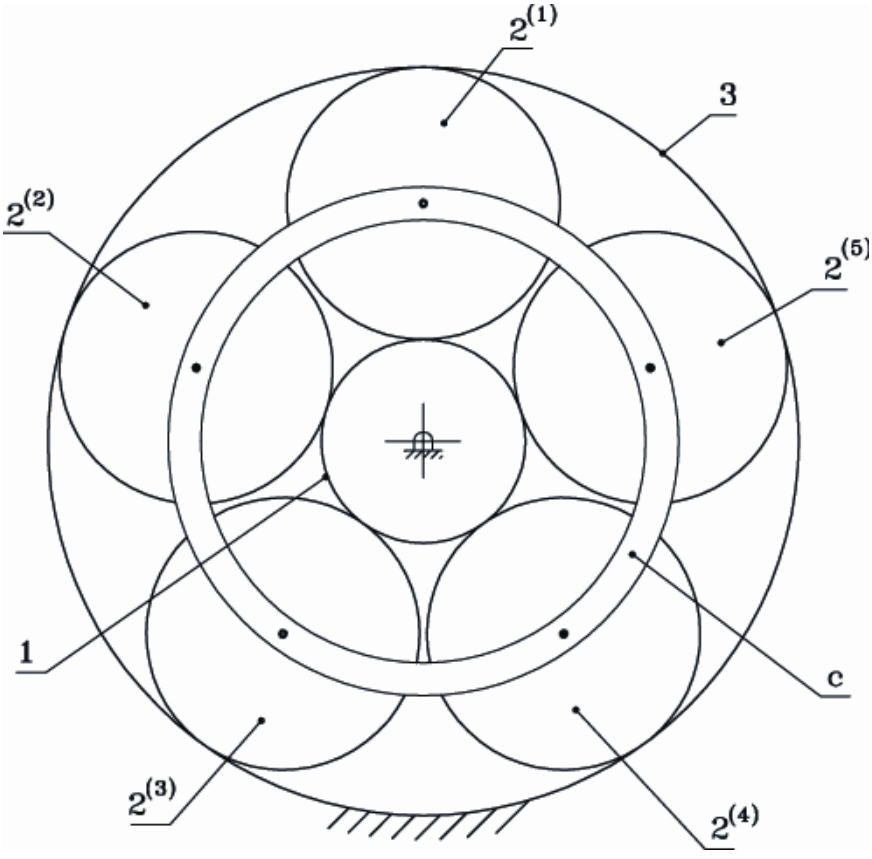

Figure 4.—Schematic representation of one stage planetary gear train.

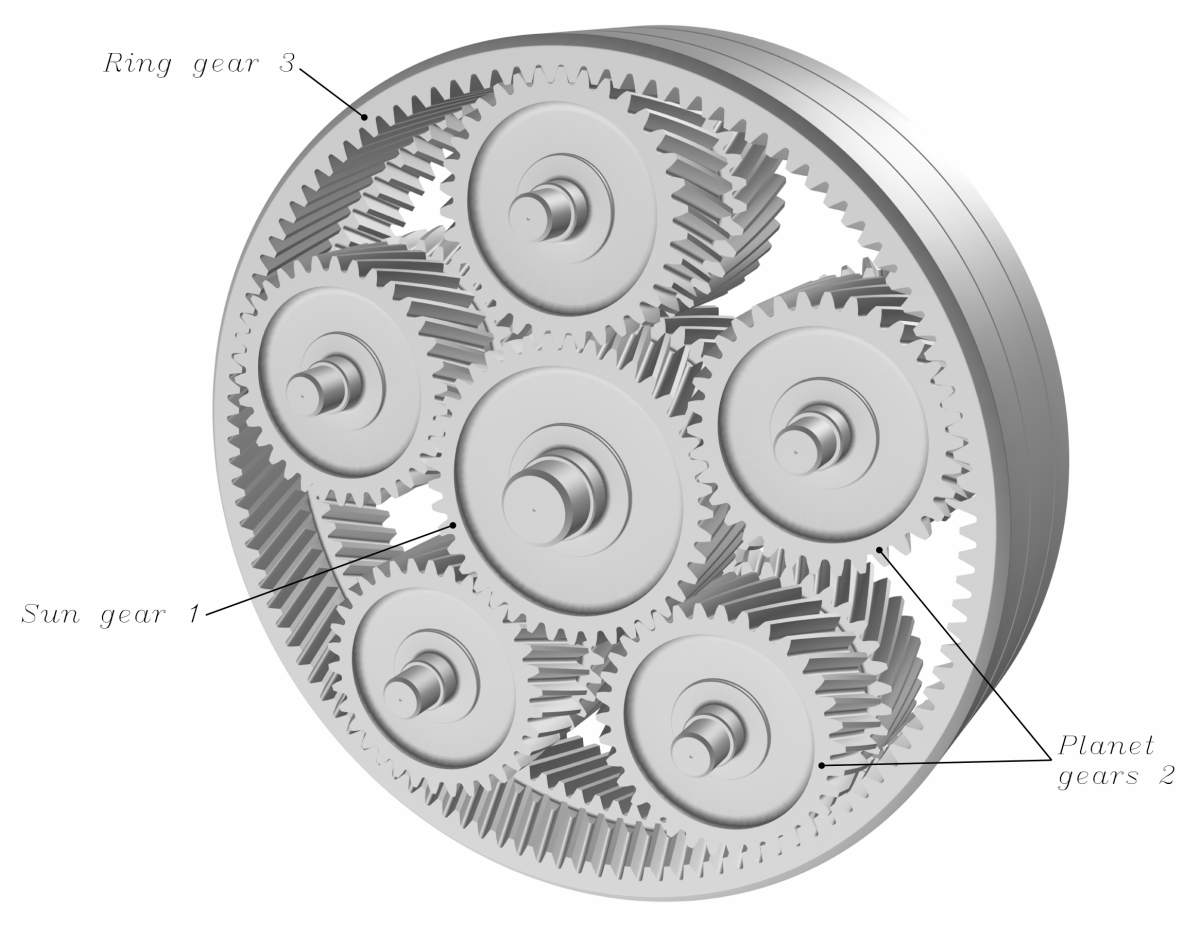

Figure 5.—Schematic of one-stage planetary gear train with double-helical gears.

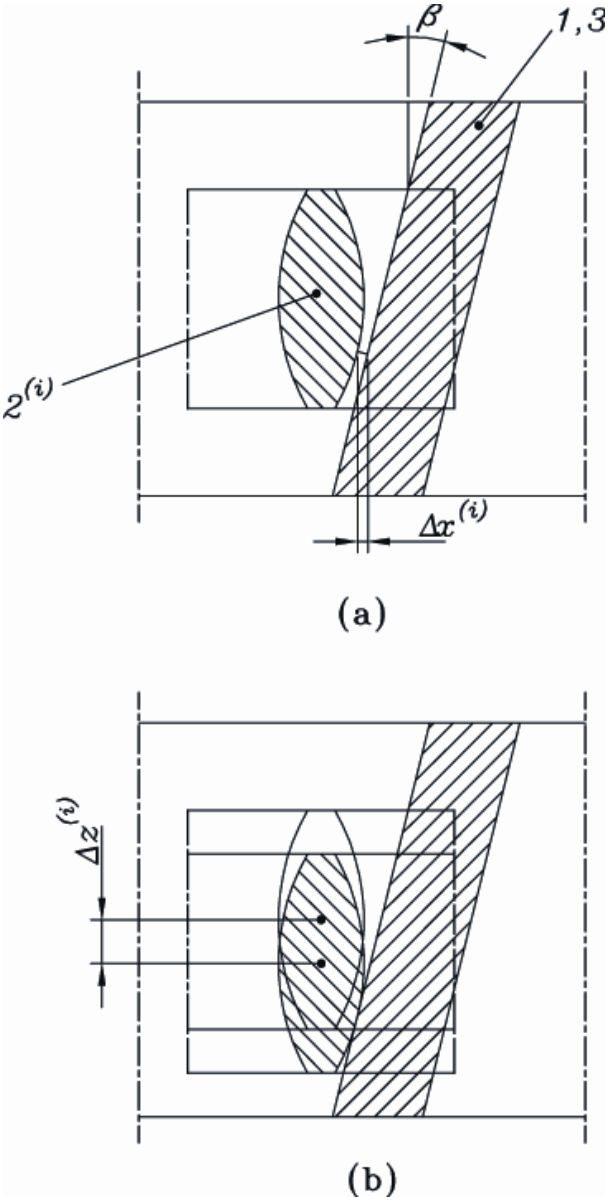

Figure 6.—Schematic illustration of regulation of backlash in one stage planetary gear train: (a) backlash between gears 1, 3, and $3^{(i)}$ before regulation; (b) elimination of backlash by axial displacement of $\Delta z^{(i)}$ of planet gear $2^{(i)}$.

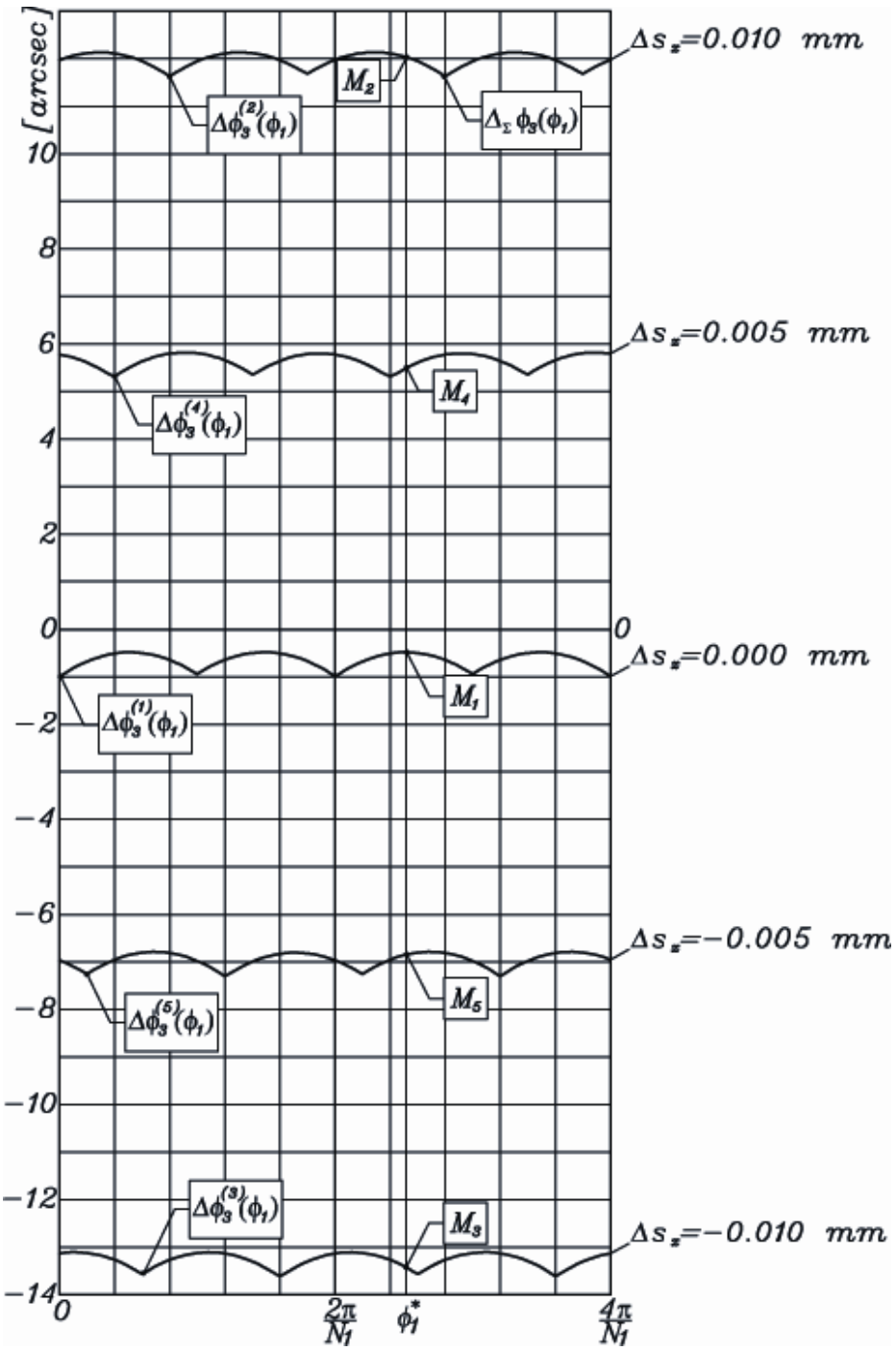

Figure 7.—Functions of transmission errors $\Delta\phi_3^{(i)}(\phi_1)$ in five subgear drives.

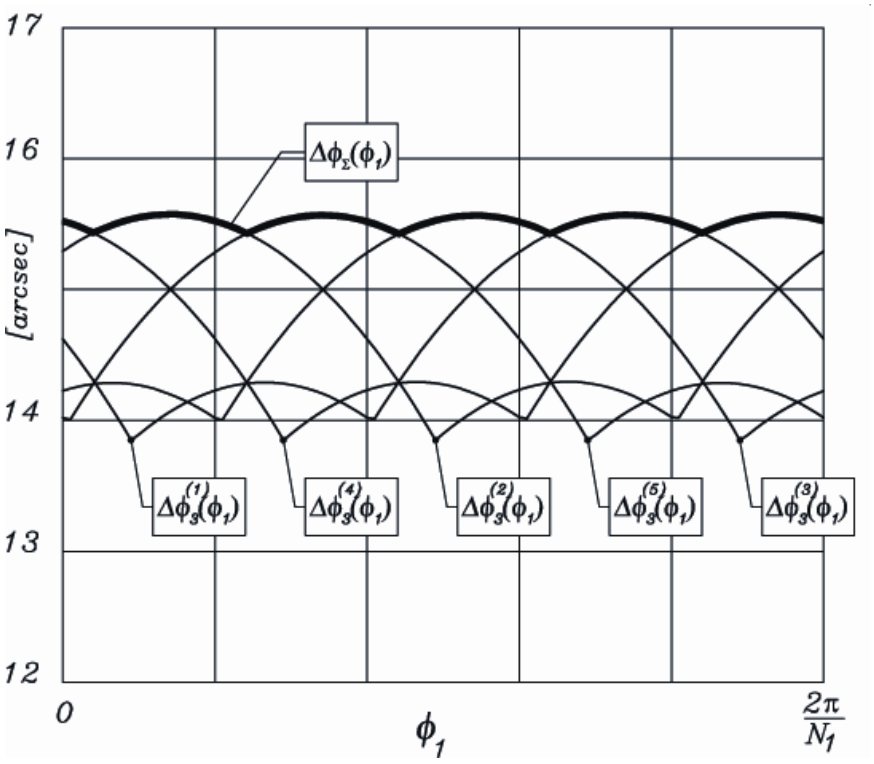

Figure 8.—Illustration of integrated functions of transmission errors for subdrives.

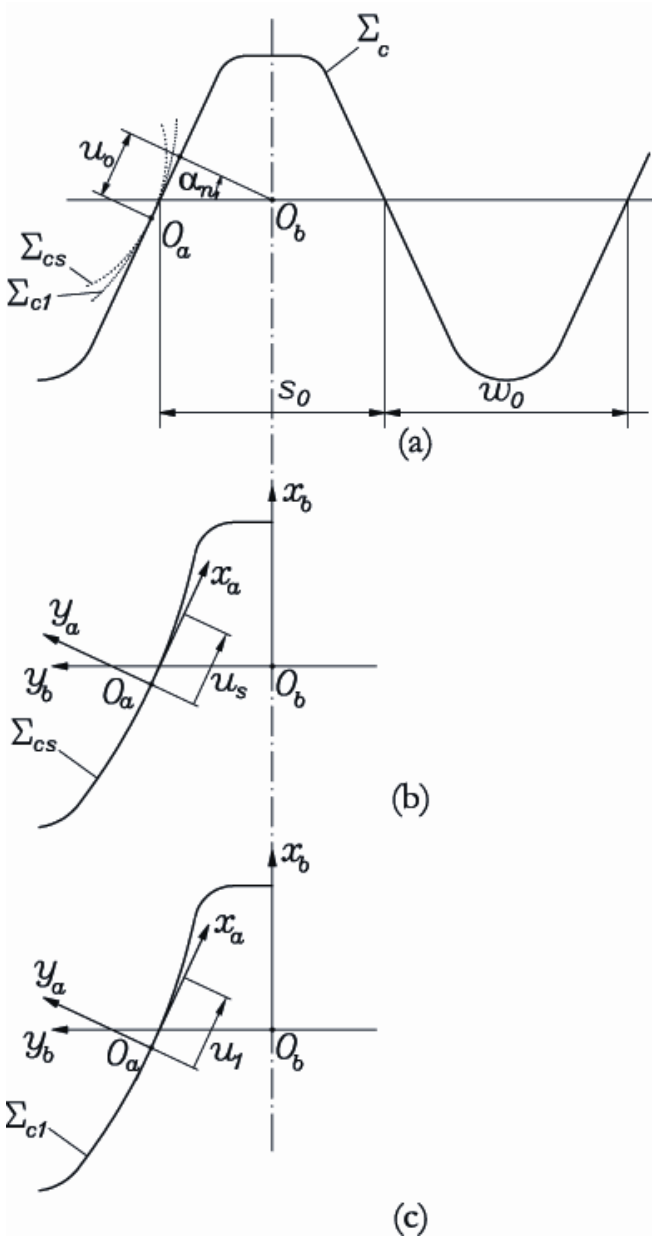

Figure 9.—Illustration of: (a) reference rack-cutter Σ_c with straight profiles, (b) shaper Σ_{cs} parabolic rack-cutter profile, (c) pinion Σ_{c1} parabolic rack-cutter profile.

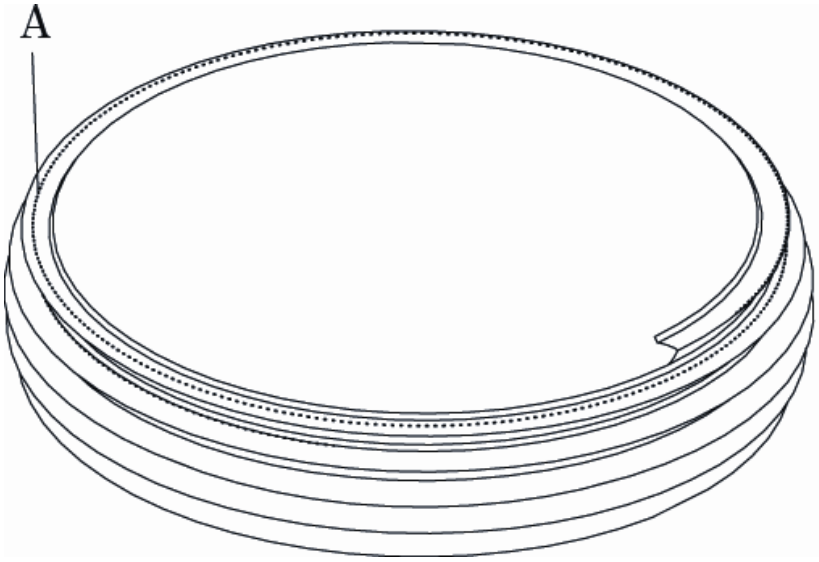

Figure 10.—Grinding (cutting) worm applied for generation of face-gear; worm singularities are indicated by A.

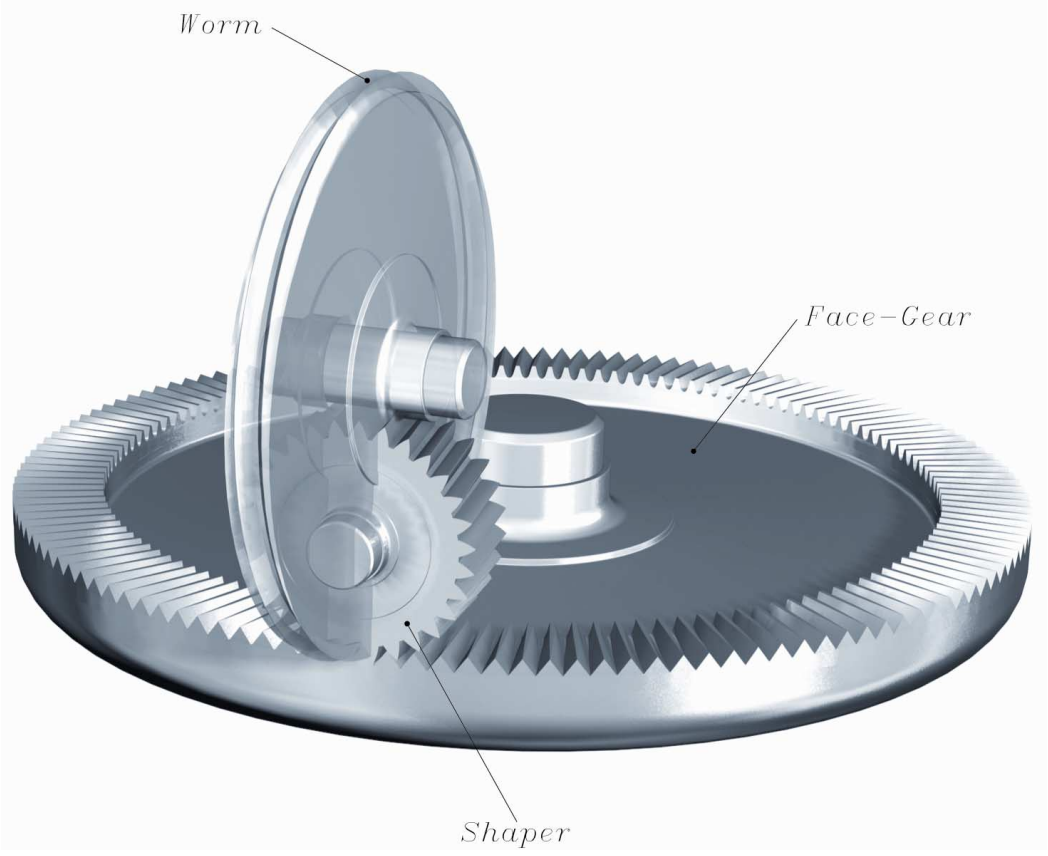

Figure 11.—Illustration of simultaneous meshing of grinding worm, shaper, and the face-gear.

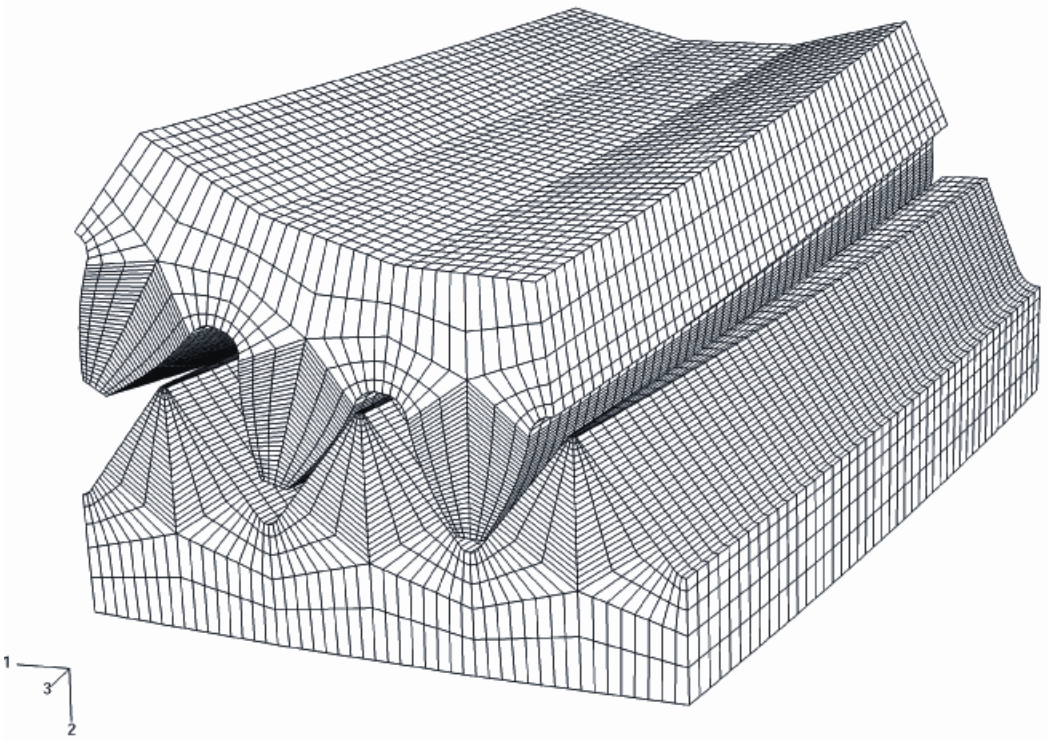

Figure 12.—Contacting model used for finite element analysis.

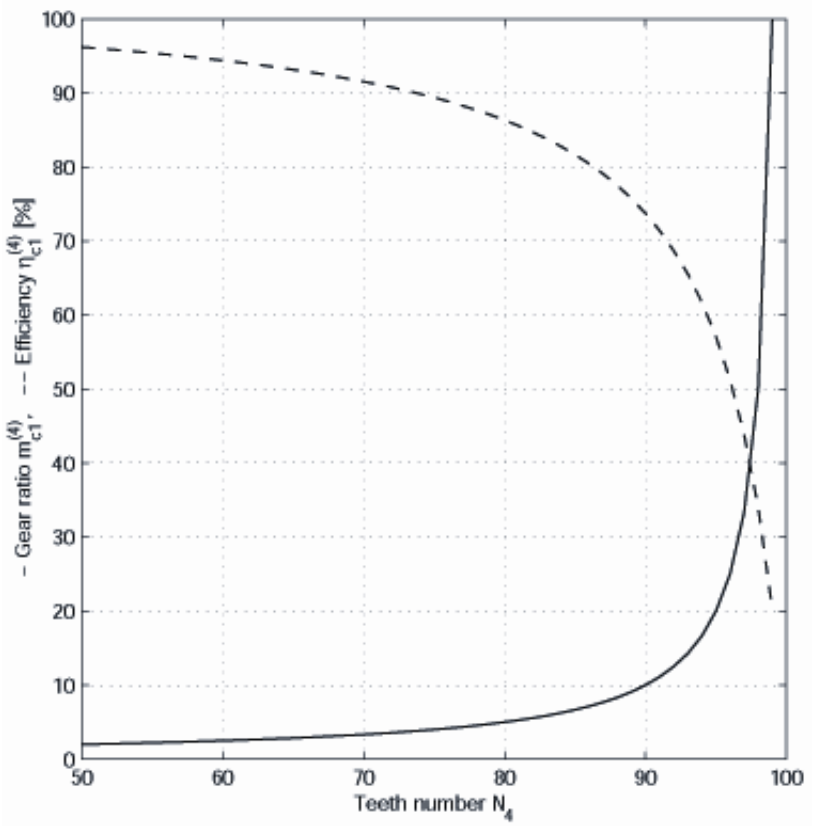

Figure 13.—Efficiency of mechanism of example 2.1.1.

REPORT DOCUMENTATION PAGE

Form Approved
OMB No. 0704-0188

1. AGENCY USE ONLY (*Leave blank*)	2. REPORT DATE	3. REPORT TYPE AND DATES COVERED
	July 2004	Final Contractor Report

4. TITLE AND SUBTITLE

New Design and Improvement of Planetary Gear Trains

5. FUNDING NUMBERS

WBS–22–714–09–15
NAG3–2450
1L162211A47A

6. AUTHOR(S)

Faydor L. Litvin, Alfonso Fuentes, Daniele Vecchiato,
and Ignacio Gonzalez-Perez

7. PERFORMING ORGANIZATION NAME(S) AND ADDRESS(ES)

University of Illinois at Chicago
Department of Mechanical and Industrial Engineering
842 W. Taylor Street
Chicago, Illinois 60607

8. PERFORMING ORGANIZATION REPORT NUMBER

E–14576

9. SPONSORING/MONITORING AGENCY NAME(S) AND ADDRESS(ES)

National Aeronautics and Space Administration
Washington, DC 20546–0001
and
U.S. Army Research Laboratory
Adelphi, Maryland 20783–1145

10. SPONSORING/MONITORING AGENCY REPORT NUMBER

NASA CR—2004-213101
ARL–CR–0540

11. SUPPLEMENTARY NOTES

Project Manger, Robert Handschuh, Vehicle Technology Directorate, NASA Glenn Research Center, organization code 0300/5950, 216–433–3969.

12a. DISTRIBUTION/AVAILABILITY STATEMENT

Unclassified - Unlimited
Subject Category: 37 Distribution: Nonstandard

Available electronically at http://gltrs.grc.nasa.gov

This publication is available from the NASA Center for AeroSpace Information, 301–621–0390.

12b. DISTRIBUTION CODE

13. ABSTRACT ***(Maximum 200 words)***

The development of new types of planetary and planetary face-gear drives is proposed. The new designs are based on regulating backlash between the gears and modifying the tooth surfaces to improve the design. The goal of this work is to obtain a nearly uniform distribution of load between the planet gears. In addition, a new type of planetary face-gear drive was developed in this project.

14. SUBJECT TERMS

Gears; Drive systems

15. NUMBER OF PAGES

31

16. PRICE CODE

17. SECURITY CLASSIFICATION OF REPORT	18. SECURITY CLASSIFICATION OF THIS PAGE	19. SECURITY CLASSIFICATION OF ABSTRACT	20. LIMITATION OF ABSTRACT
Unclassified	Unclassified	Unclassified	